



## Research article

## Tau biosensor on aptamer-modified interdigitated electrode for monitoring neurological effect caused by anesthesia

Hongjuan Gao<sup>a</sup>, Han Qin<sup>b,\*</sup>, Hongjing Fu<sup>a,\*\*</sup>, Jing Feng<sup>c</sup>, Min Chen<sup>c</sup><sup>a</sup> Operating Room, Wuhan Fourth Hospital, Wuhan, 430000, China<sup>b</sup> Department of Anesthesiology, Wuhan Fourth Hospital, Wuhan, 430000, China<sup>c</sup> Department of Nursing, Wuhan Fourth Hospital, Wuhan, 430000, China

## ARTICLE INFO

## Keywords:

Anesthesia

Tau protein

Biosensor: interdigitated electrode

Aptamer

## ABSTRACT

General anesthesia is significantly gaining prominence and becoming unavoidable in modern medicine. Since neuroprotein fluctuations are common during anesthetic procedures, it is essential to monitor protein levels to identify neuro-related issues. Tau protein fluctuations are often found in the anesthetic process, and higher levels of tau are highly related to various neuro-related issues. Researchers are focusing on monitoring tau levels during and after anesthesia. This research has developed a high-sensitive tau biosensor on a gold nanomaterial-modified interdigitated electrode, measured at 0–2 V on a dual-probe station. Aptamer and antibody were used as capture and detection molecules, and a biotin-streptavidin strategy was employed to attach a higher number of aptamers on the electrode. These immobilized aptamers recognize the tau protein and form a sandwich with antibodies, lowering the detection of tau protein to 1 fM on a linear regression from 0.001 to 100 pM ( $y = 2.0651x - 1.3813$ ,  $R^2 = 0.987$ ). Further, tau-spiked cerebrospinal fluid increases the current flow without any interferences, confirming the selective detection of tau protein.

## 1. Introduction

Anesthesia is necessary for surgery and other major medical treatments. The anesthetic procedure is more successful in modern medicine; however, the side effects caused by anesthesia are still considered a serious issue. Anesthesia can initiate and accelerate various diseases such as cardiovascular conditions, neural injury, cancer, and neurodegenerative disorders [1,2]. In particular, anesthetic procedures can lead to the development and worsening of Alzheimer's disease (AD) and Parkinson's disease (PD). AD and PD are common neurodegenerative disorders that require lifelong attention and treatment, which results in a significant financial burden on the medical industry [3–5]. In addition, patients with AD are particularly at risk of deterioration after anesthesia. Moreover, anesthesia increases the incidence of cognitive dysfunction, such as declines in learning, memory, and attention. Therefore, monitoring the condition of the patient during and after anesthesia is necessary to detect issues caused by the anesthesia. Tau protein is a microtubule-associated protein that fluctuates significantly due to the anesthesia process and is highly related to various neurological disorders [6]. The abnormal levels of tau protein affect neuron functions, which in turn affects nerve cells and leads to cognitive

\* Corresponding author.

\*\* Corresponding author.

E-mail addresses: [gaohongjuan88@sina.com](mailto:gaohongjuan88@sina.com) (H. Gao), [whdsyyqh@sina.com](mailto:whdsyyqh@sina.com) (H. Qin), [swbfhj727827@sina.com](mailto:swbfhj727827@sina.com) (H. Fu), [fj171969@sina.com](mailto:fj171969@sina.com) (J. Feng), [shangqingcheng16@sina.com](mailto:shangqingcheng16@sina.com) (M. Chen).<https://doi.org/10.1016/j.heliyon.2024.e37449>

Received 20 June 2024; Received in revised form 26 August 2024; Accepted 2 September 2024

Available online 5 September 2024

2405-8440/© 2024 Published by Elsevier Ltd.

This is an open access article under the CC BY-NC-ND license

<http://creativecommons.org/licenses/by-nc-nd/4.0/>.

function damage [7]. Therefore, monitoring the level of tau helps to identify neuro-related issues caused by anesthetic procedures. In this research, a tau biosensor was developed on a gold nanomaterial-modified interdigitated electrode sensor for monitoring the side effects caused by anesthesia.

Biosensor is the biological sensor that convert the biological interactions into an electrical signal and have been used widely for various applications [8,9]. Improving biosensor is mandatory to improve the detection of diseases at an early stage [10,11]. The early detection of diseases mainly depends on the specific and selective detections of biomolecules at the lower level with appropriate partner molecule [12]. Different biomarkers are generated for identifying diseases by using biosensor [13]. In general, sensitivity and selectivity are relying on various factors, which include the analyte and target interaction, and surface functionalization [14]. Among these, surface functionalization plays a major role in improving the limit of detection. Increasing the immobilization of capture molecules with proper orientation lowers the limit of detection. In this research, an aptamer-antibody sandwich assay was conducted for the detection of tau protein on Interdigitated electrodes (IDEs). Aptamer was utilized to capture the tau protein, so increasing the number of aptamers attached to the electrode improves tau protein detection. To enhance aptamer immobilization, a biotin-streptavidin strategy was used for surface functionalization. IDEs are widely employed in a wide range of sensing applications because of their special geometry, which permits effective electrical interactions and a large surface area. IDEs are made up of conductive material fingers that interlock when placed on a substrate. An electric field is created between the fingers when a potential difference is supplied across the electrodes. Changes in electrical characteristics like capacitance, resistance, or impedance result from this electric field's interaction with the analyte, or material being measured. The presence or concentration of the target analyte can be used to measure and correlate these changes. Sensitive and selective detection is made possible by the large surface area and the capacity to functionalize the electrodes with certain proteins.

Biotin-streptavidin has stronger binding ability and utilized for various sensors for improving the detection limit [15]. Apart from that, streptavidin has four binding regions, there is a possibility of attracting one streptavidin to three or four biotinylated aptamers, which increases the number aptamer binding on the sensing electrode. Apart from that various nanomaterials are effectively utilized for various medical purposes [16,17]. Here to enhance the aptamer immobilization, streptavidin conjugated gold nanoparticle was used for surface functionalization. Gold nanoparticles (GNPs) exhibit unique properties that can be utilized a tailored surface modification, enabling its use in medical diagnostics and biochemical sensing [18,19]. In particular, GNP-conjugated with streptavidin are used frequently for various biosensing purposes. Apart from that, surface functionalization with GNP provides better stability and arrangement of streptavidin on the sensing surfaces and binds with higher number biotinylated aptamer. Previously, it was proved that streptavidin conjugated GNP improves the anti-FIX aptamer immobilization on the silica surface and lowered the detection of target protein to 100 pM [20]. In the tau biosensor, amine and glutaraldehyde modified IDE was used to attach streptavidin-GNP, and then biotinylated aptamer was bound to streptavidin. Tau protein was further sandwiched with aptamer and antibody to identify the level of tau in the artificial CSF, which helps monitor the condition of the patient during and after anesthesia.

## 2. Materials and methods

### 2.1. Reagents and biomolecules

Tau protein, anti-tau antibody, streptavidin-GNP, Glutaraldehyde, (3-Aminopropyl)-trimethoxysilane, and PBS were ordered from Sigma Aldrich, USA. The mixture of phosphate, KCl, NaCl, CaCl<sub>2</sub>, and MgCl<sub>2</sub> was used to prepare the artificial cerebrospinal fluid (CSF) [21,22]. Tau specific DNA aptamer (5'-GCGGAGCGTGGCAGG-3') was used as the capture probe [23]. Both specific and complementary aptamer (5'-CCTGCCACGCTCCGC-3') sequences were synthesized chemically by the local supplier. Human complement factor H (CFH) and anti-CFH antibody were received from Sigma Aldrich (USA) and used for control performances. Interdigitated electrode (IDE) surface was fabricated as described earlier under optimal condition [24]. Artificial cerebrospinal fluid (CSF) was prepared by the mixture of 1 mM phosphate, 150 mM NaCl, 3.0 mM KCl and 1.4 mM CaCl<sub>2</sub>·2H<sub>2</sub>O.

Using AutoCAD software, the electrode device design was created (2 × 1 cm), with the electrode size (5 μm) with the same spacing width. The design was then printed onto a photomask. For the purpose of pattern transfer, the photomask was mounted to the chrome glass surface. A layer of silicon oxide (SiO<sub>2</sub>) at 300 Å was formed on the wafer by wet thermal oxidation. After that, Al coils were used in a thermal evaporator to deposit Al metal on the oxide layer. After the Al wafer was deposited, the substrate was electrode-patterned using a standard photolithography technique. Using a spin coater set to 2500 rpm, a positive photoresist was first applied to the wafer that had been deposited with Al. After that, the wafer was soft-baked for 1 min at 90 °C to eliminate any moisture and the sedimentary wave on the SiO<sub>2</sub> surface. Wafer was placed on the alignment stage and the chrome mask was put on the UV mask aligner. In order to transfer the IDE pattern onto the photoresist, the alignment stage was adjusted appropriately, and the UV light exposure was turned on for 10 s. To remove the photoresist in the unexposed area, the wafer is then repeatedly dipped in the photoresist developer [24].

### 2.2. Biotinylated aptamer immobilization on IDE

The anti-tau aptamer on the IDE was immobilized using the biotin-streptavidin binding strategy. To immobilize the streptavidin, the surface was first modified to introduce amine groups. APTES (2 % diluted in 30 % ethanol) was dropped onto the IDE and allowed to sit at room temperature (RT) for 2 h. Following a wash with 30 % ethanol, 2 % diluted glutaraldehyde (GLU) was applied to the APTES-modified surface and left for 1 h at room temperature. After the washing procedures, 200 nM of diluted streptavidin was applied to the surface. Additionally, 1 M ethanolamine was used to block the remaining GLU surfaces. Finally, a 1 μM biotinylated tau aptamer was applied to the surface to interact with the streptavidin. The current responses were recorded for all the surface

functionalization steps.

### 2.3. Tau protein quantification by aptamer and antibody

Tau protein was identified by an aptamer-antibody sandwich assay on IDE. Following the aptamer surface modification, 1 M ethanolamine was used to cover the excess GLU, as two aldehyde groups and potentially reacts amine group with ethanolamine. At this point, the current level was recorded. The tau protein was then diluted from 1 fM to 100 pM and placed onto an IDE with an aptamer attached. Next, 250 nM of anti-tau antibody was added to form a sandwich complex. Again, the current level was noted and compared before and after the sandwich assay. To determine the tau protein detection limit, the difference in current for each concentration was computed and recorded in an Excel sheet.

### 2.4. Identification of tau protein from artificial CSF spiked tau

To confirm the detection of tau from the biological sample, tau protein concentrations (1 fM to 100 pM) were spiked in artificial CSF and then detected by the above sandwich. Following steps are involved in this process. (i) KOH treated IDE was modified into amine by 1 % APTES; (ii) 2 % of GLU was added and rested for 1 h; (iii) 200 nM of streptavidin was introduced; (iv) 1  $\mu$ M of biotinylated aptamer was placed; (v) Surface was blocked with 1 M of ethanolamine; (vi) Tau-spiked CSF was added; (vii) 250 nM of anti-tau antibody was added. The current levels were recorded and compared before and after the sandwich assay for the comparison.

### 2.5. Biofouling experiment with control proteins

Biofouling experiments with different combinations of controls, protein CFH and complementary aptamer were conducted for the specific identification of tau protein. Experiments were conducted (i) without tau protein; (ii) without anti-tau antibody; (iii) with CFH; (iv) with anti-CFH antibody; (v) With complementary aptamer. The current levels were recorded and all the experiments compared with the specific performance. All measurements were carried out on a dual probe station at room temperature, and the sensing surface was maintained as wet using 10 mM PBS (pH 7.4). Washing was carried out between each surface modification/interaction using 10 mM PBS (pH 7.4). The power supply was from an ammeter, ranging from 0 to 2 V with a sweep of 0.1 V.

## 3. Results and discussion

Anesthesia is a mandatory procedure for various medical treatments, including surgery. The side effects caused by anesthesia can lead to various health issues. Therefore, monitoring the health condition during and after the anesthesia procedure is essential to avoid these health issues [6]. Here, a tau biosensor was developed to monitor the neurological changes during the anesthesia procedure.

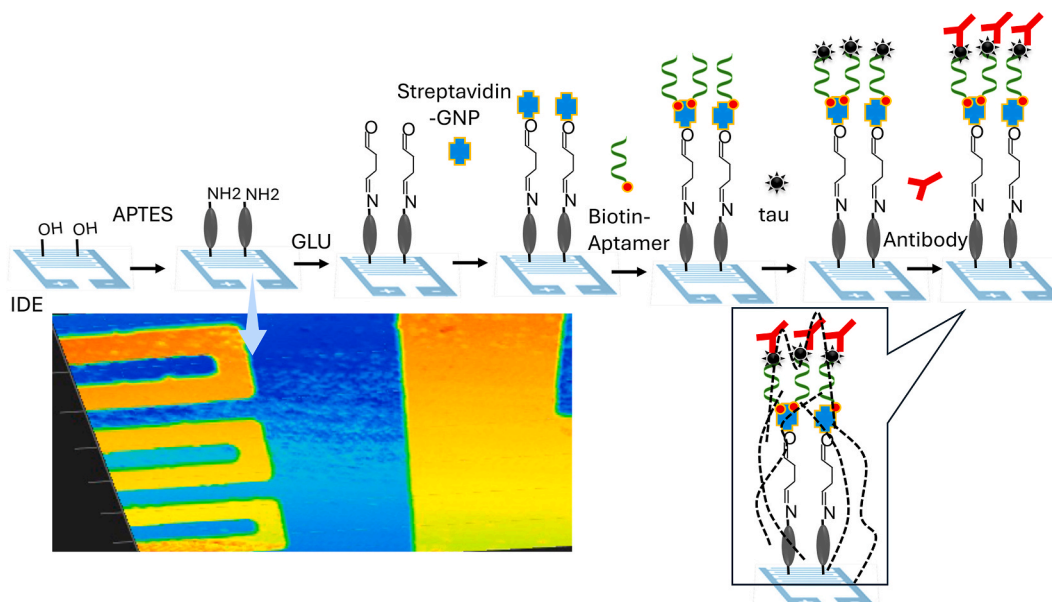


**Fig. 1.** Schematic representation of tau biosensor on IDE. IDE was hydroxylated with KOH and then amine modification conducted by APTES. GLU was further used to link the streptavidin-GNP on APTES. And then, biotinylated aptamer was immobilized on the streptavidin. Finally, Tau protein was introduced and then sandwiched by anti-tau antibody. Figure insets describe the surface structure of IDE under 3D-nanoprofiler and the surface dipole mechanism.

Fig. 1 shows the schematic representation of the tau biosensor on an interdigitated electrode sensor. Initially, the IDE was hydroxylated with KOH and then modified into amine by APTES. Researchers have shown that without OH groups, amine binding on the electrode is reduced due to the lower acceptance of hydrogen and polar bonds [25–27]. On the amine modified electrode, GLU was placed to link the streptavidin-GNP. GLU is an organic molecule found as the effective crosslinker for antibodies, peptides, and proteins [28–30]. Then, biotinylated aptamer was immobilized on the streptavidin. Since biotin and streptavidin have a high binding affinity, and streptavidin has four binding sites for biotin, it was expected that a higher number of aptamers would attach to the sensing electrode through the biotin-streptavidin interaction. On these aptamer-attached surfaces, tau protein was introduced and then sandwiched with anti-tau antibody.

### 3.1. Surface functionalization of aptamer immobilization on IDE

The anti-tau aptamer immobilization process was monitored by IDE sensor. Fig. 2 shows the current volt measurement of biotinylated aptamer immobilization process. As shown in Fig. 2a, the bare IDE shows the current as  $4.17 \text{ E}-09 \text{ A}$ , after modifying the surface into amine, the current was increased to  $6.5 \text{ E}-09 \text{ A}$ . Further, when GLU was attached, the current level was increased to  $8.45 \text{ E}-09 \text{ A}$ . On the GLU surface, streptavidin-GNP was introduced, and a drastic increment of current ( $1.68 \text{ E}-08 \text{ A}$ ) was recorded. The size of the GNP and the amount of streptavidin on the GNP enhance the current flow on IDE, which confirms the attachment of streptavidin-GNP on IDE. Further, when biotinylated aptamer was added, the current flow was increased to  $2.81 \text{ E}-08 \text{ A}$  (Fig. 2b). The amount of capture molecule on the sensing electrode is a key factor for improving the sensitivity of the target molecule. In the tau sensor, anti-tau aptamer was used to capture tau protein, and anti-tau antibody was used to detect. Since aptamer has higher binding affinity and more sensitive and selective with the target molecule, aptamer was used to capture tau protein, which helps to lower the detection level [31]. At the same time, antibody is bigger in size, and helps to increase the current flow upon binding with tau protein on the electrode. In addition, GNP provides a better arrangement of streptavidin on IDE and possible to attract higher number of aptamers and also provide the stable attachment of aptamer, which increases the attraction of higher tau protein and anti-tau antibody on IDE. This will help to increase the interaction of tau with aptamer and antibody and lower the detection limit of tau protein.

### 3.2. Quantification of tau protein by aptamer and antibody

Tau protein was identified by its aptamer and antibody on IDE. Different concentrations of tau protein was diluted and added individually on aptamer attached surfaces and then anti-tau antibody was added for sandwich detection. Fig. 3a shows the current volt graph with different concentrations of tau protein interaction with its aptamer and antibody. Before the detection, GLU was covered by ethanolamine to avoid the nonspecific binding. APTES and GLU were used for surface functionalization to attach the aptamer on IDE. When tau was added on the surface, it could possibly bind on the uncovered GLU surface and cause changes in the signal-to-noise ratio. To avoid this situation, ethanolamine was added before introducing the tau protein. As shown in Fig. 3b, the addition of ethanolamine shows the slight change of current response, this is because the most GLU surfaces were occupied by streptavidin-GNP. Further, upon adding  $0.001 \text{ pM}$  of tau protein, the current was changed from  $3 \text{ E}-08$  to  $3.57 \text{ E}-08 \text{ A}$ , which indicates the smaller interaction of tau protein with its antibody and aptamer. Further, when tau protein concentrations were increased to  $0.01, 0.1, 1, 10$  and  $100 \text{ pM}$ , current levels were increased to  $5.24 \text{ E}-08, 8.51 \text{ E}-08, 1.06 \text{ E}-07, 1.21 \text{ E}-07$ , and  $1.36 \text{ E}-07 \text{ A}$ , respectively (Fig. 3b). It was evident that raising the concentrations of tau protein caused a linear increment in current levels. The detection limit of tau protein was determined to be  $1 \text{ fM}$  with an  $R^2$  value of  $0.987$  after the current difference was computed and shown in a linear regression line (Fig. 4a). With the use of streptavidin-conjugated GNP and a higher and more stable aptamer immobilization on IDE, a substantial lower level of tau protein detection was attained. As a general fact, the size of an aptamer is much smaller ( $\sim 1000$  times) than that of an antibody. Due to its smaller size, the number of aptamer molecules captured on the sensing surface can be much higher than that of antibodies. Therefore, it is highly recommended to use aptamers as capturing molecules. When switching between capturing and detecting molecules, the sensing system still works well; however, antibodies display less sensitivity when used as capturing molecules.

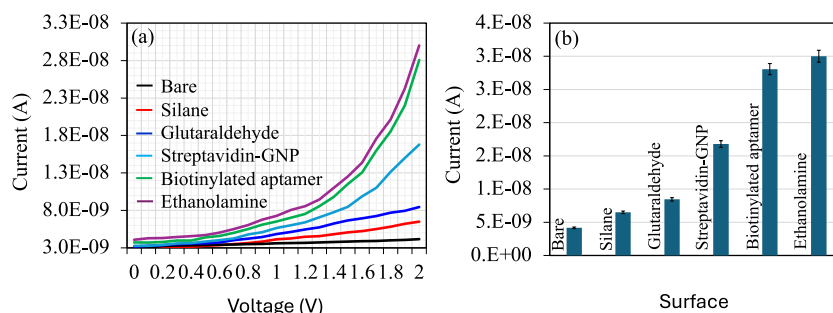
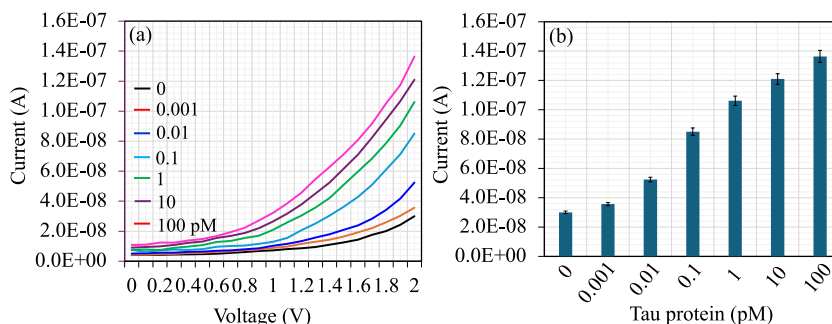
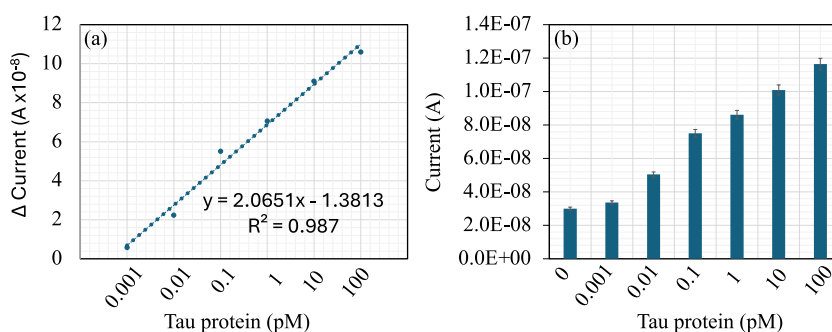


Fig. 2. Anti-tau aptamer immobilization process was monitored by IDE sensor. (a) Graph of current-volt of biotinylated aptamer immobilization. Substantial current variations were seen following in every immobilization procedure. (b) Current response of aptamer immobilization process. Current was increased after adding biotinylated aptamer and lesser difference with ethanolamine attachment was noted due to the high occupancy of aptamer. Error values indicate the mean of three independent experiments.



**Fig. 3.** Quantification of tau protein. (a) current volt graph of different concentrations of tau protein interaction with its aptamer and antibody. Substantial current variations were seen after the addition of tau protein. (b) Current level of tau protein interactions with aptamer and antibody. With increasing tau concentrations, the responses of current also increased gradually. Error values indicate the mean of three independent experiments.



**Fig. 4.** (a) Detection limit of tau protein. The current level difference for every tau protein concentration was computed and shown on a linear regression line. An  $R^2$  value of 0.987 indicates the detection limit at 1 fM. (b) Identification of tau in artificial CSF. Difference concentrations of tau were spiked in CSF and identified by tau sensor. The current responses were increased with enhancing the spiked tau protein concentrations in CSF without any interference. Error values indicate the mean of three independent experiments.

### 3.3. Identification of tau protein from artificial CSF

To confirm the detection of tau protein in biological sample, tau protein was spiked in artificial CSF and detected by the tau sensor. In general, the tau concentration at 60 pg/mL is considered to be normal in human [32]. During the aesthetic procedure, tau level was increased and causes various neurological disorders [33]. Therefore, monitoring the level of tau in the CSF is necessary to avoid the issues caused by anesthesia. To identify tau in real-life situations, different concentrations of tau were spiked in artificial CSF, dropped on aptamer-immobilized surfaces, and detected using anti-tau antibody. As shown in Fig. 4b, the current response increased with increasing concentrations of tau protein-spiked CSF. The increase in current responses without any interference indicates the specific

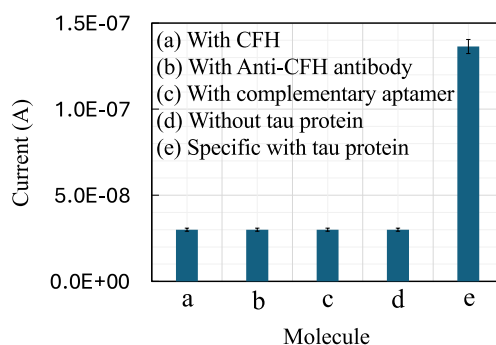


**Fig. 5.** Biofouling experiment with control protein CFH and complementary of tau aptamer for a specific detection of tau protein. Experiments were conducted, (i) without tau protein; (ii) without anti-tau antibody; (iii) with CFH; (iv) with anti-CFH antibody; (v) with complementary aptamer. There is no change of current noted, which indicated that, tau protein specially recognized by its aptamer and antibody without biofouling. Error values indicate the mean of three independent experiments.

detection of tau protein in the biological sample, helping to monitor tau levels during anesthetic procedures.

### 3.4. Biofouling with control protein and complementary aptamer

Biofouling experiment was performed with control protein, CFH and complementary of tau aptamer for the specific detection of tau protein. Experiments were conducted, (i) without tau protein; (ii) without anti-tau antibody; (iii) with CFH; (iv) with anti-CFH antibody; (v) with complementary aptamer sequence. Without anti-tau antibody, there is no interaction between tau protein and the antibody. Additionally, CFH cannot interact with tau aptamer and antibody, so no current response was recorded. Similarly, with complementary aptamer and anti-CFH antibody, tau protein cannot interact, resulting in no changes in current (Fig. 5). This result indicates that tau protein is specifically recognized by its aptamer and antibody without biofouling.

## 4. Conclusion

Anesthesia is a common procedure during surgery and other treatments in modern medicine. However, side effects can occur in some patients after the anesthetic procedure. In particular, patients with Alzheimer's disease and Parkinson's disease are especially vulnerable to side effects from general anesthesia. Therefore, monitoring the condition of the patient during and after anesthesia is necessary. This work focused on developing a tau protein biosensor for identifying neurological changes during and after anesthesia. A high number of anti-tau aptamers were attached to the interdigitated electrode through the biotin-streptavidin strategy and streptavidin-conjugated gold nanoparticles. On the biotinylated aptamer-modified surface, tau was identified by a sandwich assay with anti-tau antibody, detecting tau as low as 1 fM. Furthermore, tau-spiked artificial CSF increased the current responses with increasing tau concentration. Control experiments with CFH and anti-CFH antibody did not show any increase in current responses, indicating the specific detection of tau on the sensing electrode. This tau sandwich assay identifies low levels of tau protein and helps monitor issues caused by anesthesia. The sensing system shown in the current study works for all other clinical and non-clinical biomarkers. However, optimization is needed when modifying the surface with other materials, as it displays differences with different molecular interactions.

### Data and code availability

No data was used for the research described in the article.

### CRedit authorship contribution statement

**Hongjuan Gao:** Writing – review & editing, Writing – original draft, Investigation, Formal analysis, Data curation. **Han Qin:** Writing – review & editing, Validation, Supervision, Software, Resources, Project administration, Methodology, Funding acquisition, Conceptualization. **Hongjing Fu:** Writing – review & editing, Validation, Supervision, Software, Resources, Project administration, Investigation, Conceptualization. **Jing Feng:** Writing – review & editing, Visualization, Validation. **Min Chen:** Writing – review & editing, Visualization, Validation.

### Declaration of competing interest

The authors declare that they have no known competing financial interests or personal relationships that could have appeared to influence the work reported in this paper.

## References

- [1] R. Botney, Improving patient safety in anesthesia: a success story? *Int. J. Radiat. Oncol. Biol. Phys.* 71 (2008) S181–S186, <https://doi.org/10.1016/j.ijrobp.2007.05.095>.
- [2] H.W. Yeh, L.T. Yeh, Y.H. Chou, S.F. Yang, S.W. Ho, Y.T. Yeh, Y.T. Yeh, Y.H. Wang, C.H. Chan, C. Bin Yeh, Risk of cardiovascular disease due to general anesthesia and neuraxial anesthesia in lower-limb fracture patients: a retrospective population-based cohort study, *Int. J. Environ. Res. Publ. Health* 17 (2020) 33, <https://doi.org/10.3390/ijerph17010033>.
- [3] X. Ma, X. Wang, Y. Xiao, Q. Zhao, Retinal examination modalities in the early detection of Alzheimer's disease: seeing brain through the eye, *J Transl Int Med* 10 (2022) 185–187, <https://doi.org/10.2478/jtim-2021-0053>.
- [4] H. Chen, N. Du, L. Wang, L. Yang, A higher risk for melanoma in patients with Parkinson's disease: based on the results from National Health and Nutrition Examination Survey 2001 – 2004, *Journal of Clinical and Basic Psychosomatics* 1 (2023) 0571, <https://doi.org/10.36922/jcbp.0571>.
- [5] L. Yu, J. Jin, Y. Xu, X. Zhu, Aberrant energy metabolism in Alzheimer's disease, *J Transl Int Med* 10 (2022) 197–206, <https://doi.org/10.2478/jtim-2022-0024>.
- [6] M. Yin, D. Xu, J. Yu, S. Huang, S.C.B. Gopinath, P. Kang, Impedance spectroscopy for identifying tau protein to monitor anesthesia-based issues, *Biotechnol. Appl. Biochem.* 69 (2022) 1805–1811, <https://doi.org/10.1002/bab.2246>.
- [7] Z. Chen, S. Wang, Z. Meng, Y. Ye, G. Shan, X. Wang, X. Zhao, Y. Jin, Tau protein plays a role in the mechanism of cognitive disorders induced by anesthetic drugs, *Front. Neurosci.* 17 (2023) 1145318, <https://doi.org/10.3389/fnins.2023.1145318>.
- [8] C.T. Pan, K. Dutt, A. Kumar, R. Kumar, C.H. Chuang, Y.T. Lo, Z.H. Wen, C.S. Wang, S.W. Kuo, PVDF/AgNP/MXene composites-based near-field electrospun fiber with enhanced piezoelectric performance for self-powered wearable sensors, *Int J Bioprint* 9 (2022) 336–353, <https://doi.org/10.18063/IJB.V9I1.647>.
- [9] M.B. Kulkarni, N.H. Ayachit, T.M. Aminabhavi, Biosensors and microfluidic biosensors: from fabrication to application, *Biosensors* 12 (2022) 543, <https://doi.org/10.3390/bios12070543>.
- [10] H. Geng, S.C.B. Gopinath, W. Niu, Highly sensitive hepatitis B virus identification by antibody-aptamer sandwich enzyme-linked immunosorbent assay, *INNOV Therapeutics and Pharmacological Sciences* 5 (2023) 7–14, <https://doi.org/10.36922/tps.298>.

- [11] J. Li, Y. Hua, L. Qiao, B. Wang, X. Pang, H. Jia, Y. Yu, B. Yu, Y. Sun, X. Zhang, Y. Chen, A novel wide-band dielectric imaging system for electro-anatomic mapping and monitoring in radiofrequency ablation and cryoablation, *J Transl Int Med* 10 (2022) 264–271, <https://doi.org/10.2478/jtim-2022-0040>.
- [12] Z.Y. Dapeng Qin, Qiuping Gong, Xin Li, Yanping Gao, Subash C.B. Gopinath, Yeng Chen, Identification of Mycoplasma pneumoniae by DNA-modified gold nanomaterials in a colorimetric assay, *Biotechnol. Appl. Biochem.* (2022), <https://doi.org/10.1002/bab.2377>.
- [13] Y. Wang, K. Hou, Y. Jin, B. Bao, S. Tang, J. Qi, Y. Yang, X. Che, Y. Liu, X. Hu, C. Zheng, Lung adenocarcinoma-specific three-integrin signature contributes to poor outcomes by metastasis and immune escape pathways, *J Transl Int Med* 9 (2021) 249–263, <https://doi.org/10.2478/jtim-2021-0046>.
- [14] A. Parihar, P. Ranjan, S.K. Sanghi, A.K. Srivastava, R. Khan, Point-of-Care biosensor-based diagnosis of COVID-19 holds promise to combat current and future pandemics, *ACS Appl. Bio Mater.* 3 (2020) 7326–7343, <https://doi.org/10.1021/acsbam.0c01083>.
- [15] T. LakshmiPriya, S.C.B. Gopinath, T.-H. Tang, Biotin-streptavidin competition mediates sensitive detection of biomolecules in enzyme linked immunosorbent assay, *PLoS One* 11 (2016) e0151153, <https://doi.org/10.1371/journal.pone.0151153>.
- [16] H. Jung Jo, M. Sung Kang, H. Jeong Jang, I. Selestin Raja, D. Lim, B. Kim, D.-W. Han, Advanced approaches with combination of 2D nanomaterials and 3D printing for exquisite neural tissue engineering *Materials Science in, Addit. Manuf.* 2 (2023) 620, <https://doi.org/10.36922/msam.0620>.
- [17] P. Sarvari, P. Sarvari, Advances in nanoparticle-based drug delivery in cancer treatment, *Global Translational Medicine* 2 (2023) 394, <https://doi.org/10.36922/gtm.0394>.
- [18] I. Letchumanan, M.K. Md Arshad, S.R. Balakrishnan, S.C.B. Gopinath, Gold-nanorod enhances dielectric voltammetry detection of c-reactive protein: a predictive strategy for cardiac failure, *Biosens. Bioelectron.* 130 (2019) 40–47, <https://doi.org/10.1016/j.bios.2019.01.042>.
- [19] R. Zhang, S. Wang, X. Huang, Y. Yang, H. Fan, F. Yang, J. Li, X. Dong, S. Feng, P. Anbu, S.C.B. Gopinath, T. Xin, Gold-nanorod seeded single-walled carbon nanotube on voltammetry sensor for diagnosing neurodegenerative Parkinson's disease, *Anal. Chim. Acta* 1094 (2020) 142–150, <https://doi.org/10.1016/j.aca.2019.10.012>.
- [20] T. LakshmiPriya, Y. Horiguchi, Y. Nagasaki, Co-immobilized poly(ethylene glycol)-block-polyamines promote sensitivity and restrict biofouling on gold sensor surface for detecting factor IX in human plasma, *Analyst* 139 (2014) 3977–3985, <https://doi.org/10.1039/c4an00168k>.
- [21] L. Liu, Q. He, F. Zhao, N. Xia, H. Liu, S. Li, R. Liu, H. Zhang, Competitive electrochemical immunoassay for detection of  $\beta$ -amyloid (1-42) and total  $\beta$ -amyloid peptides using p-aminophenol redox cycling, *Biosens. Bioelectron.* 51 (2014) 208–212, <https://doi.org/10.1016/j.bios.2013.07.047>.
- [22] K. Hegnerová, M. Bocková, H. Vaisocherová, Z. Křištofiková, J. Řičný, D. Řípková, J. Homola, Surface plasmon resonance biosensors for detection of Alzheimer disease biomarker, *Sens Actuators B Chem* 139 (2009) 69–73, <https://doi.org/10.1016/j.snb.2008.09.006>.
- [23] S. Kim, A.W. Wark, H.J. Lee, Femtomolar detection of tau proteins in undiluted plasma using surface plasmon resonance, *Anal. Chem.* 88 (2016) 7793–7799, <https://doi.org/10.1021/acs.analchem.6b01825>.
- [24] A. Ghosh, S.C.B. Gopinath, S.M. Firdous, S. Ramanathan, Early detection of viral DNA in breast cancer using fingered aluminium interdigitated electrode modified by Streptavidin-biotin tetraivalent complex, *J. Indian Chem. Soc.* 99 (2022), <https://doi.org/10.1016/j.jics.2022.100604>.
- [25] S.K. Vashist, E. Marion Schneider, E. Lam, S. Hrapovic, J.H.T. Luong, One-step antibody immobilization-based rapid and highly-sensitive sandwich ELISA procedure for potential in vitro diagnostics, *Sci. Rep.* 4 (2014) 4407, <https://doi.org/10.1038/srep04407>.
- [26] S. Paraja, S.C.B. Gopinath, M.K. Md Arshad, Aptasensing Ampicillin on Silica Substrate Gapped by Interdigitated Aluminium Electrode, *Micro and Nanosystems*, 2019, <https://doi.org/10.2174/1876402911666190404151857>.
- [27] S.C.B. Gopinath, K. Awazu, M. Fujimaki, Waveguide-mode sensors as aptasensors, *Sensors* 12 (2012) 2136–2151, <https://doi.org/10.3390/s120202136>.
- [28] S.C.B. Gopinath, K. Awazu, M. Fujimaki, K. Shimizu, Evaluation of anti-A/Udorn/307/1972 antibody specificity to influenza A/H3N2 viruses using an evanescent-field coupled waveguide-mode sensor, *PLoS One* 8 (2013) e81396, <https://doi.org/10.1371/journal.pone.0081396>.
- [29] I. Migneault, C. Dartiguenave, J. Vinh, M.J. Bertrand, K.C. Waldron, Comparison of two glutaraldehyde immobilization techniques for solid-phase tryptic peptide mapping of human hemoglobin by capillary zone electrophoresis and mass spectrometry, *Electrophoresis* 25 (2004) 1367–1378, <https://doi.org/10.1002/elps.200305861>.
- [30] C. Wang, T. LakshmiPriya, S.C.B. Gopinath, Amine-aldehyde chemical conjugation on a potassium hydroxide-treated polystyrene ELISA surface for nanosensing an HIV-p24 antigen, *Nanoscale Res. Lett.* 14 (2019) 21.
- [31] Jian Luo, Subash C.B. Gopinath, Sreeramanan Subramaniam, Zaifeng Wu, Arthritis biosensing, Aptamer-antibody-mediated identification of biomarkers by ELISA, *Process Biochem.* 121 (2022) 396–402.
- [32] N. Möhn, Y. Luo, T. Skripuletz, P. Schwenkenbecher, I. Zerr, P. Lange, M. Stangel, Tau-protein concentrations are not elevated in cerebrospinal fluid of patients with progressive multifocal leukoencephalopathy, *Fluids Barriers CNS* 16 (2019) 28, <https://doi.org/10.1186/s12987-019-0148-3>.
- [33] Y. Dong, X. Wu, Z. Xu, Y. Zhang, Z. Xie, Anesthetic isoflurane increases phosphorylated tau levels mediated by caspase activation and A $\beta$  generation, *PLoS One* 7 (2012) e39386, <https://doi.org/10.1371/journal.pone.0039386>.